Monte—Carlo model of the diffusion-limited reaction kinetics in microheterogeneous media. Comparison with the experimental plots of the forward and backward electron phototransfer kinetics on the pore diameter in silica gel

G. A. Vinogradov and P. P. Levin★

N. M. Emanuel´ Institute of Biochemical Physics, Russian Academy of Sciences, 4 ul. Kosygina, 119991 Moscow, Russian Federation. Fax: +7 (095) 137 4101. E-mail: levinp@sky1.chph.ras.ru

The kinetics of the diffusion-limited decay reaction A + B → B was simulated by the Monte—Carlo method on a two-dimensional square lattice with defects presented by randomly distributed sites. The cases were considered where [B] ≫ [A] at the random initial distribution (quenching reaction) and [B] = [A] with the initial distribution of the A and B particles on neighboring sites (geminate recombination). The kinetic curves were approximated by the simplest analytical equation $[A]/[A]_0 = (1 - \varphi)\exp[-(kt)^{1-h}] + \varphi$ (where k and φ are constants). The plots of the heterogeneity parameter (h) and time-averaged first-order rate constant *vs*. concentration of defects (p) or B particles (in the case of quenching) were obtained and compared with similar correlations obtained earlier by the experimental study of the kinetics of forward (quenching reaction) and backward (geminate recombination) electron phototransfer on the surface of different porous silica gels. The experimental plots of h *vs.* silica gel porosity are in satisfactory agreement with the plots of h *vs.* p in the model space, if the fraction of volume inaccessible for reactants, calculated from the free silica gel volume, is chosen as the p parameter for silica gel.

Key words: Monte—Carlo method, fractal, dimensionality of space, diffusion-limited reaction, quenching, geminate recombination, electron phototransfer, silica gel, pore diameter.

The kinetics of diffusion-limited bimolecular reactions in disordered, low-dimensional, and fractal media does not obey the classical kinetic laws.[1—9] The kinetic behavior of the simplest pseudo-monomolecular reaction of particle decay on traps differs for the three- (3D) and two-dimensional (2D) spaces. In the so-called "gas" approximation when the filling of the space with particles and traps (q) is much lower than unity, the probability of particle survival ($w(t)$) in the 2D space at rather short times with the logarithmic accuracy has the form

$$w(t) \approx \exp\{-[qt/\ln(1/q)]\},$$

which differs from the decay kinetics for the 3D space[1]

$$w(t) \approx \exp(-qt).$$

The asymptotic behavior at long times ($t \to \infty$) for spaces with different dimensionalities also differs

$$w(t) \approx \exp[-(qt)^{1/2}],$$
$$w(t) \approx \exp[-(q^{2/3}t)^{3/5}]$$

in the cases of 2D and 3D,[2] respectively. Fluctuations of trap densities in spaces with different dimensionalities should be taken into account to correctly describe the asymptotic behavior of the probability of particle decay.[2,3] The importance of taking into account fluctuations for description of various physicochemical phenomena has been considered in detail elsewhere.[4]

The kinetic laws describing bimolecular processes reflect the initial spatial distribution of reacting particles and their subsequent spatial and reaction dynamics. The influence of the space dimensionality on the kinetic regularities is evidently caused by the difference in the intensity of diffusion "stirring" of reactants and by different topological restrictions (organization of space). Diffusion is restricted in spaces with an effective dimensionality lower than 3D, *i.e.*, the Einstein law is violated

$$\langle r^2 \rangle = Dt,$$

where r is the displacement from the initial position (in the case, naturally, $\langle r \rangle = 0$), and D is the diffusion coefficient. From the viewpoint of formal kinetics, this results in kinetic laws where the reaction rate constant is time-dependent. Exact analytical data are lacking and, therefore, one has to use numerical simulation for theoretical

Published in Russian in *Izvestiya Akademii Nauk. Seriya Khimicheskaya,* No. 8, pp. 1536—1541, August, 2004.

1066-5285/04/5308-1596

analysis, while approximate expressions should be used to process experimental results.

In the case of the diffusion-limited reaction A + B → B at [B] ≫ [A] and the random initial distribution of reactants (photochemical quenching reactions), the decay kinetics of the A particles in the space with a dimensionality lower than three is theoretically described by the series

$$[A](t)/[A]_0 = \exp(-C_1 t^{1-h} + C_2 t^{2(1-h)} - C_3 t^{3(1-h)} + ...), \quad (1)$$

where $0 \le h \le 1$, $[A]_0$, C_1, C_2, C_3, *etc*. are constants; in particular, h is the so-called heterogeneity constant related to the space geometry.[10,11] The exponent of Eq. (1) contains the sign-variable series, which imposes rigid restrictions on the constant values C_1, C_2, C_3, *etc*. Experimental kinetic curves of fluorescence decay in the presence of a quencher in disordered media with microreactors, such as micelles, microemulsions, and vesicles, are satisfactorily described, in many cases, by Eq. (1) containing the first term or two first terms in the exponent.[11—14]

To describe the kinetics of various processes in disordered media, the following empirical expression is widely used:

$$[A](t)/[A]_0 = (1 - \varphi)\exp[-(k_f t)^{1-h}] + \varphi, \quad (2)$$

where k_f, $0 \le h \le 1$, and φ are constants.[11—19] The φ parameter takes into account both experimental features of the system (for instance, the presence of residual absorbance or luminescence of other, longer-lived, or intermediate products) and a possible contribution of other terms in the exponent in Eq. (1). The corresponding plot of the effective rate constant of the first-order reaction *vs.* time ($k(t)$) is described as follows:

$$k(t) = (1-h)k_f^{1-h}t^{-h}. \quad (3)$$

Polychromatic kinetic curves, which are satisfactorily described by law (2), are experimentally observed for both chemical reactions and various processes of physical relaxation (in particular, mechanical or dielectric) in many microheterogeneous disordered media, such as glasses and polymers.[6,15] The time dependence of the rate constant can be caused by both spatial and energy heterogeneity.

We successfully used Eq. (2) for adequate description of the kinetics of diffusion-limited quenching of the triplet states of quinones *via* the electron transfer from aromatic amines and the geminate recombination (backward electron transfer) of the corresponding radical ion pairs on the surface of several varieties of porous silica gels.[16—19] The heterogeneity constant (h) was established to depend substantially on the silica gel structure and to increase with an increase in its porosity.[17]

Since analytical expressions capable of predicting the kinetics of bimolecular reactions in disordered spaces with a specified geometry are lacking, one has to use numerical simulation methods, among which the Monte—Carlo (MC) method is the most efficient. Lattice models are most popular among various procedures for MC calculation of the kinetics of bimolecular reactions. According to these models, particles involved in reactions are randomly wandering over sites of the correspondingly organized lattice.[11,13,14,20]

In this work, the MC method was used to calculate the kinetics of the diffusion-limited reactions A + B → B for [B] ≫ [A] and the random initial distribution of the reactants (quenching reaction), as well as for [B] = [A] and the pairwise initial localization of A and B on neighboring sites (geminate recombination) for a two-dimensional square lattice with chaotically arranged defects, *i.e.*, the sites forbidden for both A and B reactants. The results of calculations were compared with the experimental kinetics of the forward (quenching) and backward (geminate recombination) electron phototransfer on silica gels with different pore diameters[16—19] and in the narrow-pored glass.[21—24]

Calculation procedure

The silica gel surface was simulated by a method similar to that used previously for other microheterogeneous disordered media.[11,13,14,20] Sites, which will further be forbidden for the reacting particles A and B, are chosen randomly, with a specified concentration on the two-dimensional square lattice of 200×200 sites. The fraction of defects (p) varies within $0 \le p \le 0.5$ for the percolation threshold at $p = 0.41$.[11] The reaction particles A and quencher molecules B are randomly distributed on thus created surface containing defects. In the case of simulation of the quenching reaction, the mutual distribution of the A and B particles is not correlated, and the condition $[B] \ge 100[A]$, $[B] \ll 1$ is fulfilled, where [A] and [B] are the fractions of sites occupied by the A and B molecules, respectively. For simulation of the geminate recombination, the A particles are distributed randomly on the free sites of the lattice, and the B particles occupy one of the four neighboring free sites. In this case, $[A] = [B] \ll 1$. The B particles are further considered to be fixed in both models, and the A particles are randomly wandering over the lattice. It is accepted that the probability of transfer of the A particles to one of the adjacent sites is 1/4 regardless of the number of free adjacent sites.

In the MC methods, the time is not usually introduced explicitly but is measured in arbitrary units ($\Delta t_h = 1$ time unit) and considered as proportional to the number of MC increments. In addition to thus defined "uniform" time, we used another approach when the time, distributed according to the Poisson law

$$\Delta t_P = \lambda\exp(-\lambda t)$$

with the mean jump time $\langle\Delta t_P\rangle = 1/\lambda$, is ascribed to each elementary MC increment. To match the times in the kinetic plots calculated for the uniform and Poisson distributions, the corresponding times were re-normed by the equation $t_h = \lambda t_P$. It turned out that the results are virtually independent of the

method used for determination of the time of interstitial transition. Therefore, all results are presented hereinafter for the Poisson time distribution at $\lambda = 1$.

The reaction act is considered as accomplished if the A particle at some time moment is found on the same site with the B particle due to wandering, and this corresponds to the same MC trajectory. To obtain reliable statistical results, averaging was performed over 10^5—10^6 MC trajectories, and the root-mean-square error did not exceed 1% of the calculated value.

The kinetic curves calculated by the MC method were approximated by Eq. (2). Thus, the plots of h and the time-averaged first-order rate constant $\langle k \rangle$ calculated from the first moment of function (3), *vs.* p were obtained

$$\langle k \rangle = (1 - h)k_f/\Gamma[1/(1 - h)], \quad (4)$$

where Γ is the gamma function. In the case of the quenching reaction, the plots of h *vs.* [B] were additionally obtained.

Results and Discussion

Kinetics of the quenching reaction. The MC-simulated plots of the A concentration *vs.* time (the number of MC increments) for the quenching reaction A + B → B in the interval of the effective conversion ([A] − φ) from 0 to 0.9 are satisfactorily described by Eq. (2), and φ takes noticeable values (≥0.01) only at $p \geq 0.3$ (Fig. 1). The kinetic curves differ substantially from monoexponential curves even for a two-dimensional lattice without defects, because for $p = 0$ the observed h value ranges from 0.12 to 0.17, depending on the B concentration. At the same time, Eq. (2) cannot exactly describe the kinetic curves at deeper conversions. The h and φ fitting parameters, which

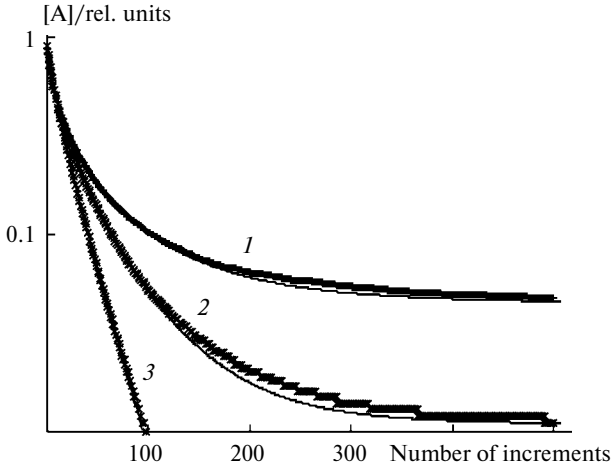

Fig. 1. Monte—Carlo kinetics of decay of the A particles in the reaction A + B → B at [B] = 0.1, [A] = 0.001, and the fraction of forbidden sites $p = 0.4$ (*1*), 0.3 (*2*), and 0 (*3*). Lines correspond to approximation by Eq. (2), $k_f = 0.055$ (*1*), 0.055 (*2*), and 0.064 (time of MC increment)$^{-1}$ (*3*); $h = 0.42$ (*1*), 0.34 (*2*), and 0.17 (*3*); φ = 0.045 (*1*), 0.011 (*2*), and 0 (*3*).

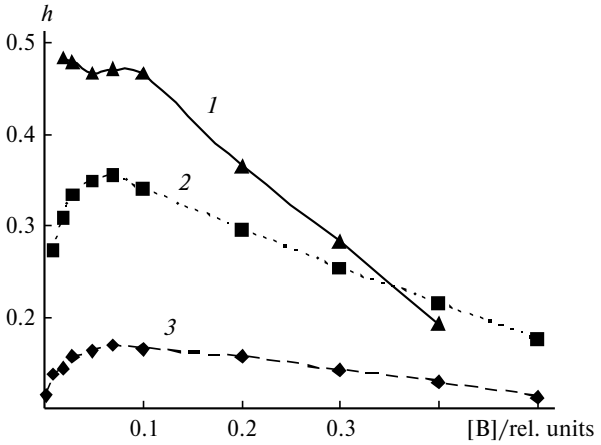

Fig. 2. Plots of the calculated heterogeneity parameter (h) *vs.* concentration of the B particles, obtained by the approximation of the corresponding kinetic curves consisting of 1000 MC increments by Eq. (2), at $p = 0.5$ (*1*), 0.3 (*2*), and 0 (*3*).

are obtained by approximation using Eq. (2), can depend (at fairly high p) on the time interval chosen for the approximation.

The observed dependence of the heterogeneity parameter (h) on the B concentration (Fig. 2) also exhibits incomplete adequacy to Eq. (2) for description of the simulated kinetic curves, while the h value is assumed to be a characteristic of the space geometry for the given type of reactions in the framework of the theory of random wandering. The h value, obtained by using Eq. (2), depends on [B] even at low p when φ = 0, Eq. (2) describes well the whole kinetic curve up to high conversions, and h is almost independent of the time interval chosen for approximation. It is of interest that the observed dependence of h on [B] passes through a maximum at [B] = 0.07 for all p which are lower than the percolation threshold ($p = 0.41$).

At the same time, the h value obtained using Eq. (2) increases, as expected, with an increase in p, *i.e.*, with an increase in the microheterogeneity of the space (Fig. 3). Compare the plots of h *vs.* p in a model space with the experimental dependences of h on the characteristics of silica gel obtained on analyzing the kinetic curves with "tail" of triplet state quenching on the surface of silica gels with different pore sizes (diameters from 2.2 to 100 nm) using Eq. (2).[16,17] One has to choose a parameter for silica gels that would be similar to the fraction of defects in the model space. Porous silica gels are chaotic aggregates of spherical particles of amorphous SiO_2 with a controlled size, which determines the surface area per weight unit and the diameter of pores formed upon spherical particle adhesion.[25] One of the most important characteristics of porous silica gels is the free (internal) volume, which is also related to the size of spherical particles forming silica gel. The chaotic structure of porous silica gels

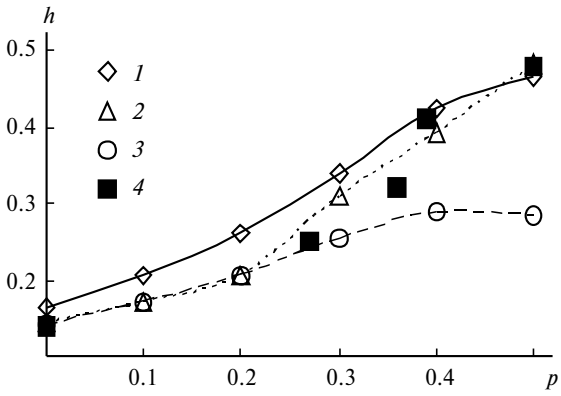

Fig. 3. Plots of the heterogeneity parameter (h) *vs.* fraction of forbidden sites (p) on the lattice, obtained by the approximation of the MC-kinetic curves of quenching by Eq. (2), at [B] = 0.1 (*1*), 0.02 (*2*), and 0.3 (*3*) and the dependence of the experimental h values on the forbidden volume fraction in silica gels with a mean pore diameter of 100, 14, 6, 4, and 2.2 nm (*4*).[15,16]

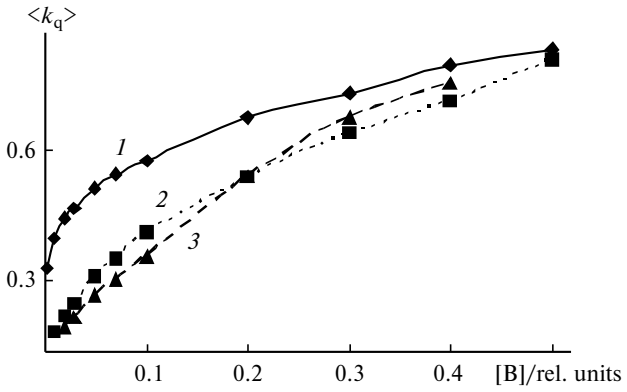

Fig. 4. Plots of the averaged quenching rate constant (<k_q>) *vs.* concentration of the B particles obtained using Eq. (4) and the approximation of the corresponding kinetic curves by Eq. (2) at p = 0 (*1*), 0.3 (*2*), and 0.5 (*3*).

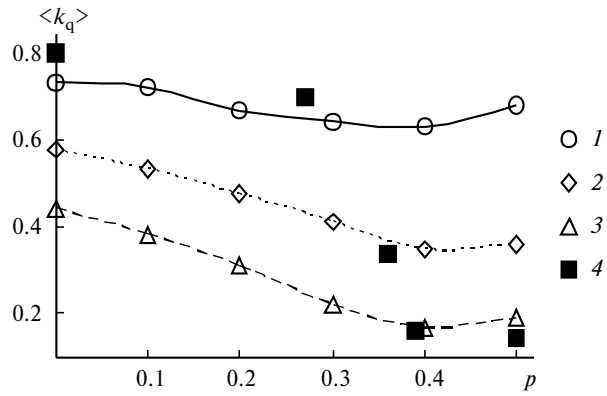

Fig. 5. Plots of the averaged quenching rate constant (<k_q>) *vs.* fraction of forbidden sites (p) on the lattice, obtained by the approximation of the corresponding kinetic curves by Eq. (2), at [B] = 0.3 (*1*), 0.1 (*2*), and 0.02 (*3*) and the properly scaled dependence of the experimental <k_q> values on the forbidden volume fraction in silica gels with a mean pore diameter of 100, 14, 6, 4, and 2.2 nm (*4*).[15,16]

suggests that the forbidden volume fraction (1 minus the free volume fraction) can serve as an analog for the fraction of forbidden sites in the model space. In fact, the dependence of the experimental h value on the forbidden volume fraction corresponds well to the plots of h *vs.* p for the model space (see Fig. 3). Thus, it seems highly probable that the macrocharacteristics of silica gel can be used as a measure of its microstructure, which determines the specific features of trajectories of molecular processes, in particular, diffusion of adsorbed molecules.[26]

A dependence of the kinetic parameters on the quencher concentration is significant for studying the kinetics of quenching reactions. In the three-dimensional space available for chaotically distributed reactants, the decay of the A particles in excess B particles is described by a monoexponential law with the rate constant increasing linearly with an increase in the B concentration. This makes it possible to obtain the rate constant of the bimolecular reaction A + B from the slope of the corresponding plot. However, in the case of a space with a lower dimensionality, an attempt to use the <k> value (see Eq. (4)) as an analog of the first-order rate constant for decay of the A particles results in a substantially nonlinear dependence of <k> on [B]. The corresponding quenching rate constant (the second-order reaction A + B) <k_q> is equal to <k>/[B] and increases with an increase in [B] (Fig. 4). Correspondingly, the plots of <k_q> *vs.* p obtained at different [B] do not coincide but reflect the general tendency of decreasing the quenching efficiency with an enhancement of the space heterogeneity. A similar trend was observed for analysis of the experimental data on the kinetics of quenching of triplet states on the surface of silica gels with different pore diameters using Eq. (2) (Fig. 5).[16,17] However, the experimental plots of <k_q> *vs.* forbidden volume fraction differ noticeably from the model curves. Evidently, the efficiency of diffusion of molecules adsorbed on the real porous surface is determined by the chemistry of surface, *e.g.*, the concentration of silanol groups, rather than by the surface geometry only.[17]

Note that the experimental plots of the average rate constant of decay of the triplet states on the silica gel surface *vs.* concentration of the co-adsorbed quencher were approximated by a linear law, although the known experimental data[17] indicate the deviation from linearity toward increasing <k_q> with an increase in the quencher concentration.

Kinetics of geminate recombination. The MC-simulated kinetic curves of geminate recombination are shown in Fig. 6. The initial region exhibiting the sharpest changes in [A] is satisfactorily described by Eq. (2). The φ values,

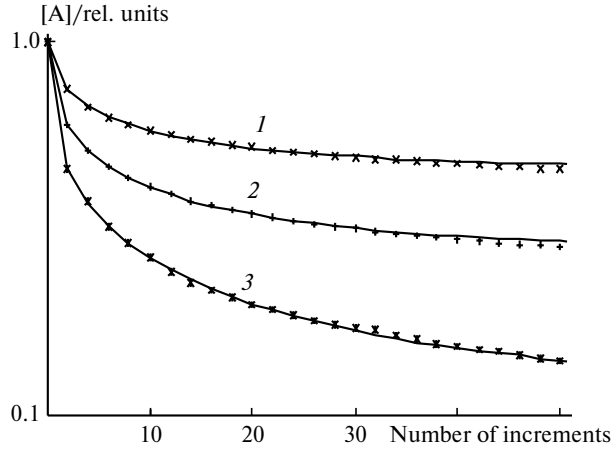

Fig. 6. MC kinetics of decay of the A particles *via* geminate recombination at the fraction of forbidden sites $p = 0$ (*1*), 0.2 (*2*), and 0.4 (*3*). Lines correspond to approximation by Eq. (2), $k_f = 0.21$ (*1*), 0.30 (*2*), and 0.41 (time of MC increment)$^{-1}$ (*3*); $h = 0.47$ (*1*), 0.55 (*2*), and 0.62 (*3*); $\varphi = 0.45$ (*1*), 0.27 (*2*), and 0.41 (*3*).

which were obtained by the approximation of the MC kinetic curves by Eq. 2, decrease and h increase with the p increase. The plots of h *vs.* p for the model space and the dependences of the experimental h values on the forbidden volume fraction in silica gel, obtained by analysis of geminate recombination on the surface of silica gels with different pore diameters,[16—19] are in a poorer agreement than those in the case of quenching; however, the characters of the experimental and calculated plots coincide (Fig. 7). The kinetics of geminate recombination on the microporous glass surface in similar systems is described

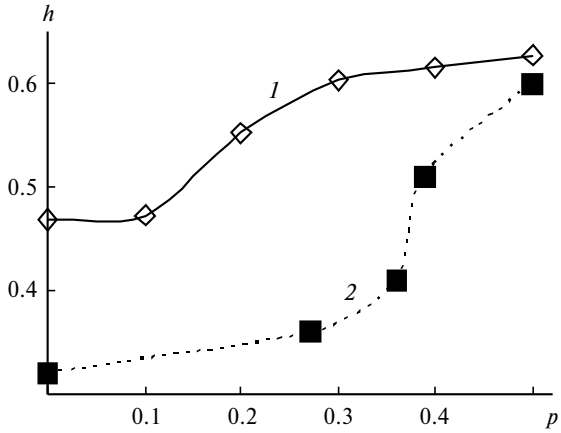

Fig. 7. Plot of the calculated heterogeneity parameter (h) *vs.* fraction of forbidden sites (p) on the lattice obtained by the approximation of the geminate recombination kinetic curves by Eq. (2) (*1*) and the dependence of the experimental h value on the forbidden volume fraction in silica gels with a mean pore diameter of 100, 14, 6, 4, and 2.2 nm (*2*).[15,16]

by Eq. (2), and the h values range from 0.3 to 0.4,[23,24] the h values in this interval being much lower than h obtained by the corresponding approximation of the MC data on a planar surface without defects. Unlike quenching, the experimentally studied geminate recombination of radical pairs born in the triplet state is controlled by diffusion and also includes the spin evolution and kinetically controlled process of the so-called intersystem recombination.[16—19,21—24] The transition from diffusion to kinetic control is accompanied by a decrease in h, which explains quantitative discrepancies between the experimental and simulated data on the geminate recombination kinetics.[16]

It should be mentioned in conclusion that a good agreement between the experimental data and results of numerical calculations was obtained for the diffusion-limited quenching reaction. This suggests that the Monte—Carlo simulation of the kinetics of diffusion-limited reactions in microheterogeneous disordered spaces with a complex dimensionality is appropriate for the quantitative description of experimental data on the basis of real parameters of porous media. This study revealed a relationship between the macrocharacteristics of the porous material (free volume, surface area) and parameters of diffusion motion of adsorbed molecules.

This work was financially supported by the Russian Foundation for Basic Research (Project Nos 02-02-16205 and 03-03-32159), the Program of the Division of Chemistry and Materials Science of the Russian Academy of Sciences "Theoretical and Experimental Investigation of the Nature of Chemical Bonding and Mechanisms of the Most Important Chemical Reactions," the Program of the Presidium of the Russian Academy of Sciences "Fundamental Problems of Physics and Chemistry of Nanodimensional Systems and Nanomaterials" (Project No. 417), and the Program of the Presidium of the Russian Academy of Sciences "Low-dimensional Quantum Structures (Project No. 9.21).

References

1. G. V. Ryazanov, *Teor. Mat. Fizika* [*Theoretical Mathematical Physics*], 1972, **10**, 271 (in Russian).
2. B. Ya. Balagurov and V. G. Vaks, *Zh. Eksp. Teor. Fiz.*, 1973, **65**, 1939 [*J. Exp. Theor. Phys.*, 1973, **65** (Engl. Transl.)].
3. A. A. Ovchinnikov and Ya. B. Zeldovich, *Chem. Phys.*, 1978, **28**, 215.
4. A. A. Ovchinnikov, S. F. Timashev, and A. A. Belyi, *Kinetika diffuzionno-kontroliruemykh khimicheskikh protsessov* [*Kinetics of Diffusion-Controlled Chemical Processes*], Khimiya, Moscow, 1986, 246 pp. (in Russian).
5. R. Kopelman, *Science*, 1988, **241**, 1620.
6. *The Fractal Approach to Heterogeneous Chemistry: Polymers, Colloids, Surfaces*, Ed. D. Avnir, Wiley, Chichester, 1989, 241 pp.

7. *Molecular Dynamics in Restricted Geometries*, Eds J. Klafter and J. M. Drake, J. Wiley and Sons, New York, 1989, 263 pp.
8. M. Sheintuch, *Catal. Rev.*, 2001, **43**, 233.
9. R. Metzler and J. Klafter, *Phys. Rep.*, 2000, **339**, 1.
10. J. Klafter and A. Blumen, *J. Chem. Phys.*, 1984, **80**, 875.
11. P. Lianos and P. Argyrakis, *J. Phys. Chem.*, 1994, **98**, 7278.
12. P. Lianos, S. Modes, G. Staikos, and W. Brown, *Langmuir*, 1992, **8**, 1054.
13. P. Argyrakis, G. Duportail, and P. Lianos, *J. Chem. Phys.*, 1991, **95**, 3808.
14. P. Lianos and P. Argyrakis, *Phys. Rev. A*, 1989, **39**, 4170.
15. W. Siebrand and T. Wildman, *Acc. Chem. Res.*, 1986, **19**, 238.
16. P. P. Levin, S. M. B. Costa, and L. F. Vieira Ferreira, *J. Phys. Chem.*, 1995, **99**, 1267.
17. P. P. Levin, S. M. B. Costa, and L. F. Vieira Ferreira, *J. Phys. Chem.*, 1996, **100**, 15171.
18. P. P. Levin, L. F. Vieira Ferreira, S. M. B. Costa, and I. V. Katalnikov, *Chem. Phys. Lett.*, 1992, **193**, 461.
19. P. P. Levin, S. M. B. Costa, and L. F. Vieira Ferreira, *Photochem. Photobiol. A: Chem.*, 1994, **82**, 137.
20. P. Argyrakis and R. Kopelman, *J. Phys. Chem.*, 1989, **93**, 225.
21. P. P. Levin, I. V. Katalnikov, and V. A. Kuzmin, *Izv. Akad. Nauk SSSR. Ser. Khim.*, 1989, 1202 [*Bull. Acad. Sci. USSR, Div. Chem. Sci.*, 1989, **38**, 1095 (Engl. Transl.)].
22. P. P. Levin, V. A. Kuzmin, and I. V. Katalnikov, *Khim. Fiz.* [*Chemical Physics*], 1989, **8**, 1604 (in Russian).
23. P. P. Levin, I. V. Katalnikov, and V. A. Kuzmin, *Chem. Phys. Lett.*, 1990, **167**, 73.
24. P. P. Levin, I. V. Katalnikov, and V. A. Kuzmin, *Chem. Phys.*, 1991, **154**, 449.
25. R. K. Iler, *The Chemistry of Silica, Solubility, Polymerization, Colloid and Surface Properties, and Biochemistry*, J. Wiley, New York, 1979, 312 pp.
26. J. J. Mecholsky, J. K. West, and D. E. Passoja, *Phylos. Magazine A*, 2002, **82**, 3163.

Received July 23, 2003;
in revised form December 19, 2003